



ELSEVIER

Available online at www.sciencedirect.com

SCIENCE @ DIRECT®

Physica A 325 (2003) 455–476

PHYSICA A

www.elsevier.com/locate/physa

Large amplitude spatial fluctuations in the boundary region of the Bose–Einstein condensate in the Gross–Pitaevskii régime

J.A. Tuszyński^{a,*}, J. Middleton^a, S. Portet^a, J.M. Dixon^b,
O. Bang^c, P.L. Christiansen^c, M Salerno^d

^a*Department of Physics, University of Alberta, Edmonton, Alta., Canada T6G 2J1*

^b*Department of Physics, The University of Warwick, Coventry CV4 7AL, UK*

^c*Institute of Mathematical Modelling, Building 305, Technical University of Denmark, DK-2800 Lyngby, Denmark*

^d*Department of Physical Sciences “E R Caianiello”, University of Salerno, Baronissi, Italy*

Received 22 January 2003

Abstract

The Gross–Pitaevskii régime of a Bose–Einstein condensate is investigated using a fully non-linear approach. The confining potential first adopted is that of a linear ramp. An infinite class of new analytical solutions of this linear ramp potential approximation to the Gross–Pitaevskii equation is found which are characterised by pronounced large-amplitude oscillations close to the boundary of the condensate. The limiting case within this class is a nodeless ground state which is known from recent investigations as an extension of the Thomas–Fermi approximation. We have found the energies of the oscillatory states to lie above the ground state energy but recent experimental work, especially on spatially confined superconductors, indicates that such states may be easily occupied and made manifest at finite temperatures. We have also investigated their stability using a Poincaré section analysis as well as a linear perturbation approach. Both these techniques demonstrate stability against small perturbations. Finally, we have discussed the relevance of these quasi-one-dimensional solutions in the context of the fully three-dimensional condensates. This has been argued on the basis of numerical work and asymptotic approximations. © 2003 Elsevier Science B.V. All rights reserved.

Keywords: Bose–Einstein condensation; Gross–Pitaevskii approximation; Superfluidity; Painlevé transcendents

* Corresponding author. Fax: +1-780-492-0714.

E-mail address: jtus@phys.ualberta.ca (J.A. Tuszyński).

1. Introduction

The theoretical prediction that a gas of non-interacting bosons below a certain critical temperature exhibits macroscopic occupation of a single quantum state was made more than 70 years ago [1,2]. Bose–Einstein condensation is known to occur in the superfluid state of liquid ^4He which had first been suggested by Fritz London in 1938 [3] and experimentally investigated using neutron scattering measurements in the 1970s and 1980s [4]. The observation of Bose–Einstein condensation (BEC) in magnetically trapped atomic vapours of rubidium [5], sodium [6] and lithium [7] has opened a new field of study involving both atomic and condensed matter physics. At present, Bose condensates are produced routinely in laboratories, which enable researchers to study, both experimentally and theoretically, condensate properties such as collective excitations [8] and interactions between two adjacent condensates [9].

The concept of Bose–Einstein condensation finds applications in many systems other than liquid ^4He . In particular, clouds of spin-polarised alkali atoms or atomic hydrogen have been utilised. They include superconducting metals where the Cooper pairs of opposite-spin and opposite momentum electrons form a Bose–Einstein condensate. However, the properties of superconductors are quantitatively very different from those of a weakly interacting gas of bosons. There are a number of open questions on the theoretical and experimental front and they include: (a) the kinetics of condensate formation, (b) the effects of interatomic interactions; (c) the role of a finite number of particles; and (d) the non-linearities and their effects on the spectrum of quantum excitations in higher spatial dimensions.

Our main interest in describing the Bose–Einstein condensate is to pay great attention to the non-linearities which are brought about by the presence of interparticle interactions. Whilst perturbative studies may adequately account for the physical situation at low concentrations, it is dubious that an equally satisfying case may be made at intermediate to high concentrations and especially for treatments requiring finite volumes. The motivation for this paper is to carefully examine the nature of fully non-linear solutions of the underlying equations of motion for the Bose–Einstein condensate. While analytical solutions are not generally feasible, they can be obtained under special conditions. In particular, we will show in this paper that close to the condensate’s boundary, the equation of motion is completely solvable and its analytical solution are amenable to physical analysis.

2. The Gross–Pitaevskii equation

The main framework for a non-linear model of Bose–Einstein condensates can be attributed to Gross [10] and Pitaevskii [11] who, working in the 1960s on Hartree-like approximations, independently obtained an energy functional for the lowest-energy inhomogeneous wavefunction, ϕ , of the condensate, which takes the form

$$E(\phi) = \int d^3\mathbf{r} \left[\frac{\hbar^2}{2m} |\nabla\phi(\mathbf{r})|^2 + V_{\text{ext}}(\mathbf{r})|\phi(\mathbf{r})|^2 + (g/2)|\phi(\mathbf{r})|^4 \right], \quad (2.1)$$

where V_{ext} is the external potential and g is a measure of the interaction strength. A more sophisticated starting Hamiltonian, which leads eventually to the form of $E(\phi)$ in Eq. (2.1), can be represented, in terms of a quantum field $\hat{\psi}$, by

$$\hat{H} = \int d^3r \hat{\psi}^\dagger \left(-\frac{\hbar^2}{2m} \nabla^2 + V_{ext} \right) \hat{\psi} + \frac{1}{2} \iint d^3r d^3r' \hat{\psi}^\dagger(\mathbf{r}) \hat{\psi}^\dagger(\mathbf{r}') V(\mathbf{r} - \mathbf{r}') \hat{\psi}(\mathbf{r}') \hat{\psi}(\mathbf{r}) \tag{2.2}$$

where the field, $\hat{\psi}$, is defined by

$$\hat{\psi} = \sum_{\alpha} \psi_{\alpha}(\mathbf{r}) \hat{a}_{\alpha} , \tag{2.3}$$

where \hat{a}_{α} is the annihilator of a state $|\alpha\rangle$ and a non-interacting Hamiltonian, H_0 , has been denoted by

$$H_0 = -\frac{\hbar^2}{2m} \nabla^2 + V_{ext} . \tag{2.4}$$

In the mean field approximation

$$\hat{\psi}(\mathbf{r}, t) \simeq \phi(\mathbf{r}, t) + \hat{\psi}'(\mathbf{r}, t) . \tag{2.5}$$

In Eq. (2.5), $\phi(\mathbf{r}, t)$ is a c -number field defined by its expectation value as

$$\phi(\mathbf{r}, t) = \langle \hat{\psi}(\mathbf{r}, t) \rangle \tag{2.6}$$

and $\hat{\psi}'(\mathbf{r}, t)$ is the quantum (non-commuting part of the field) component.

For a dilute gas we replace $V(\mathbf{r}' - \mathbf{r})$ by

$$V(\mathbf{r}' - \mathbf{r}) = g\delta(\mathbf{r}' - \mathbf{r}) \tag{2.7}$$

where $g = 4\pi\hbar^2 a/m$, a being the scattering length of S-waves. Thus by using the mean field approximation, as in Eq. (2.6), the equation of motion becomes

$$i\hbar \frac{\partial \phi}{\partial t} = -\frac{\hbar^2}{2m} \nabla^2 \phi + V_{ext} \phi + g|\phi|^2 \phi \tag{2.8}$$

which is the Gross–Pitaevskii (GP) equation.

The validity of Eq. (2.8) is based on the following two conditions:

- i. $N \gg 1$ where N is the number of atoms in the condensate; and
- ii. $a \ll$ the average distance between atoms.

For $g < 0$ the coupling is attractive whereas if $g > 0$ it denotes a repulsive interaction. Strictly speaking the GP equation is valid only in the zero temperature limit

although it has recently been amply demonstrated that its validity is much wider than this [12]. This form is in the spirit of Landau–Ginzburg formalism and hence has been shown to be more than an adequate description of a vast array of critical phenomena. Consequently, its applicability beyond the zero Kelvin limit as well as to higher energy states is meaningful and warranted. For example, the solution of the GP equation which does not correspond to the lowest energy may be statistically populated as the temperature is increased above 0 K.

It is of great interest that the GP equation for the condensate takes the form of the stationary generalised non-linear Schrödinger equation (NLS) which has been the subject of intense investigations in mathematical and non-linear physics for the past 25 years or so [13]. A standard approach for solving the GP equation is to assume that

$$\phi(\mathbf{r}, t) = A(\mathbf{r}, t) \exp(-i\mu t/\hbar), \quad (2.9)$$

where μ is the chemical potential (if $T = 0$) and $A(\mathbf{r})$ is real and normalised to the total number of particles, N , i.e.,

$$\int A^2(\mathbf{r}) d^3\mathbf{r} = N. \quad (2.10)$$

The GP equation then becomes

$$\left(-\frac{\hbar^2}{2m} \nabla^2 + V_{ext} + gA^2(\mathbf{r}) \right) A(\mathbf{r}) = \mu A(\mathbf{r}) \quad (2.11)$$

with particle density, $n(\mathbf{r})$, given by

$$n(\mathbf{r}) = |\phi(\mathbf{r}, t)|^2 = A^2(\mathbf{r}). \quad (2.12)$$

For large values of the scattering length, or conversely the number of particles in the trap is large enough, ignoring the kinetic energy in the GP equation provides a suitable approximation in the interior region of the condensate. This leads to the Thomas–Fermi approximation yielding the wavefunction, $A(\mathbf{r})$, so that

$$A(\mathbf{r}) = \left[\frac{m}{4\pi\hbar^2 a} (\mu - V_{ext}(\mathbf{r})) \right]^{1/2} = A_{TF}. \quad (2.13)$$

From the normalisation for the above function, we have that

$$N \simeq 4\pi \int_0^R r^2 |A_{TF}|^2 dr = \frac{2}{15} \frac{m\alpha}{\hbar^2 a} (\mu/\alpha)^{5/2}, \quad (2.14)$$

where R is defined by $\mu = V_{ext}(R)$ and for simplicity we write $V_{ext} = \alpha r^2$. Thus, we obtain an approximate relationship between the number of particles, N , and the chemical potential, μ , as

$$\mu = \left[\frac{15}{2} \frac{\hbar^2 a}{m} N \alpha^{3/2} \right]^{2/5}. \quad (2.15)$$

Therefore, μ scales with $N^{2/5}$.

3. The linear ramp approximation

In three dimensions, assuming spherical symmetry, the GP equation takes the form

$$-\frac{\hbar^2}{2m} \frac{d^2\psi}{dr^2} - \frac{\hbar^2}{mr} \frac{d\psi}{dr} + (V - \mu)\psi + \frac{4\pi\hbar^2 a}{m} \psi^3 = 0, \tag{3.1}$$

where μ is the chemical potential which can be treated as an adjustable parameter determining the normalisation of the condensate to a given number of particles. We will not consider orbital angular momentum in this context although its effect has been discussed in the literature, see for example Ref. [14].

Since the boundary region poses a special challenge where the role of non-linearity may be particularly significant and the condensate inhomogeneous giving rise to large spatial fluctuations, we will seek solutions of the GP equation in this vicinity, i.e., when $r \simeq R$ such that

$$\mu \simeq V_{ext}(R). \tag{3.2}$$

Taking as a most common example a parabolic confining potential of the form

$$V_{ext}(\mathbf{r}) = \alpha r^2, \tag{3.3}$$

we readily find that the boundary radius is given by

$$R = \sqrt{\mu/\alpha}. \tag{3.4}$$

For r near the boundary the confining potential, $V_{ext}(\mathbf{r})$, can be expanded in a Taylor series giving

$$W = V - \mu \simeq F(r - R), \tag{3.5}$$

where

$$F = 2\sqrt{\mu\alpha}. \tag{3.6}$$

We also introduce

$$\xi = (r - R)/d, \tag{3.7}$$

where

$$d = \left(\frac{2m}{\hbar^2} F \right)^{-1/3}.$$

The substitution $\psi = P/r$ in Eq. (3.1) conveniently removes the single gradient term and multiplication by r gives an equation of the form of Eq. (3.1) with ψ replaced by P , the first gradient term missing and the parameter a changed to a/r^2 . We are interested in the region near the condensate boundary so we approximate

$$a/r^2 \simeq a/R^2 = \tilde{a}$$

The dependent field variable is now scaled according to

$$\psi(r) = \frac{1}{d\sqrt{8\pi\tilde{a}}} \phi(\xi) \tag{3.8}$$

and we obtain the reduced equation in the form

$$\phi'' - (\xi + \phi^2)\phi = 0. \quad (3.9)$$

Following Thomas and Fermi, a very approximate asymptotic solution of Eq. (3.9) has been found by Dalfovo et al. [15] and is given by

$$\phi \simeq \sqrt{-\xi}. \quad (3.10)$$

This solution describes the condensate inside the boundary region since it ignores the kinetic energy and, as the latter authors demonstrated, agrees well with the numerical solution especially for large numbers of particles. Furthermore, this is a smooth function of the distance to the boundary showing no effect of spatial fluctuations that may be expected due to thermal agitation.

We may now compare Eq. (3.9), that represents an approximate spherically symmetric three-dimensional equation, with the corresponding equation in one dimension for the linear ramp potential. In one dimension the GP equation in this case takes the form

$$\left\{ -\frac{\hbar^2}{2m} \frac{d^2}{dx^2} + Fx + U_0 |\psi(x)|^2 \right\} \psi(x) = 0. \quad (3.11)$$

We scale the dependent and independent variables in Eq. (3.11) by writing

$$y = x/\delta, \quad \phi = \psi/b, \quad (3.12)$$

where

$$\delta = (\hbar^2/2mF)^{1/3} \quad (3.13)$$

and

$$b = (F/U_0)^{1/2} (\hbar^2/2mF)^{1/6}. \quad (3.14)$$

The constant U_0 is defined by

$$U_0 = 4\pi\hbar^2 a/m \quad (3.15)$$

and with the above scalings we obtain the dimensionless equation for the wavefunction

$$\phi'' = y\phi + \phi^3. \quad (3.16)$$

Thus the approximation of a one-dimensional ramp potential can be justified to represent the spherically symmetric three-dimensional condensate wavefunction by a linear expansion of the potential in the vicinity of the condensate's boundary.

4. Non-linear solution of the field equations

It is indeed very fortunate that Eq. (3.9) has, in the past, been thoroughly investigated by a number of mathematicians [16–18] and its solutions have been identified

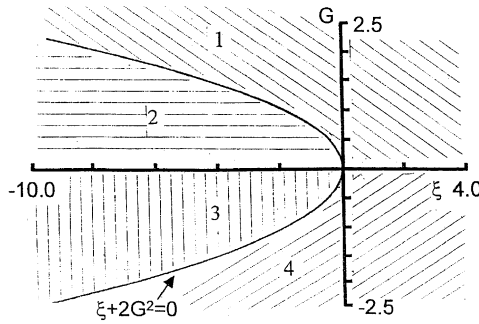


Fig. 1. Division of the (ξ, G) plane into 4 regions for solutions of Eq. (4.1).

as belonging to the Second Painlevé Transcendent class of special functions [19]. In order to bring Eq. (3.16) into standard form we write $\phi = \sqrt{2}G$ so that Eq. (3.16) becomes

$$G'' = \xi G + 2G^3. \tag{4.1}$$

Following Rosales [17] the (ξ, G) plane can be divided into four regions: (1) $G > 0, \xi + 2G^2 > 0$; (2) $G > 0, \xi + 2G^2 < 0$; (3) $G < 0, \xi + 2G^2 < 0$; (4) $G < 0, \xi + 2G^2 > 0$. Any solution $G = G(\xi)$ of Eq. (4.1) will be strictly concave in regions (1) and (4) and strictly convex in the other two regions (see Fig. 1). What this means is that the solutions of physical interest must be entirely contained within the two branches of the parabola $\xi = 2G^2$ for negative ξ . It so happens that the solutions analysed in Ref. [15] do not satisfy the above criterion and hence are divergent, though they have been normalised by truncating their domain to a small region of negative ξ thereby saving their physical relevance. However, as demonstrated by Refs. [16,17] there exists an infinity of well behaved physically acceptable solutions to Eq. (4.1) which merit a detailed analysis and this is the goal which we pursue in this paper.

First of all, Hastings and McLeod [20] demonstrated that the linearised solution of Eq. (4.1) behaves asymptotically as

$$G(\xi) \simeq Ai(\xi) \sim \pi^{-1/2} |\xi|^{-1/4} \cos \left\{ \frac{2}{3} |\xi|^{3/2} - \frac{\pi}{4} \right\} \quad \text{as } \xi \rightarrow -\infty \tag{4.2}$$

and

$$G(\xi) \simeq Ai(\xi) \sim \frac{1}{2} \pi^{-1/2} \xi^{-1/4} \exp \left\{ -\frac{2}{3} \xi^{2/3} \right\} \quad \text{as } \xi \rightarrow +\infty \tag{4.3}$$

and the Airy functions, $Ai(\xi)$, are obviously well behaved in the entire domain. More importantly perhaps Clarkson and McLeod [18] proved a theorem which states that any solution of the fully non-linear equation, i.e., Eq. (4.1), with the condition $G \rightarrow 0$ as $\xi \rightarrow +\infty$, is asymptotic to $kAi(\xi)$, where $-1 < k < 1$, and labels the continuum of non-singular solutions of our equations uniquely (Fig. 2). Furthermore, the same

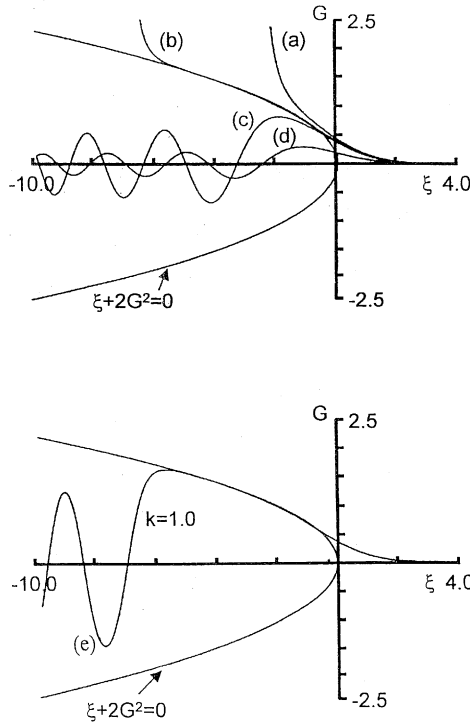


Fig. 2. Family of solutions of Eq. (4.1) with different values of k . (a) $k = 1.1$, (b) $k = 1.0 + 10^{-6}$, (c) $k = 0.95$, (d) $k = 0.5$, (e) $k = 1.0$.

authors obtained a very accurate formula for the non-linear solution given by

$$G_k(\xi) \sim d|\xi|^{-1/4} \sin \left\{ \frac{2}{3}|\xi|^{3/2} - \frac{3}{4}d^2 \ln|\xi| - c \right\} \tag{4.4}$$

as $\xi \rightarrow -\infty$. It was also demonstrated by Clarkson and McLeod [18] that the parameters c and d in Eq. (4.4) are given in terms of k only, as

$$d^2(k) = -\pi^{-1} \ln(1 - k^2) \tag{4.5}$$

and

$$c(k) = \frac{3}{2}d^2 \ln 2 + \arg \left\{ \Gamma \left(1 - \frac{1}{2}id^2 \right) \right\} - \frac{\pi}{4}. \tag{4.6}$$

In Fig. 3 we have shown a comparison between the approximation in Eq. (4.4) and the linearisation in Eq. (4.2) and the Airy function corresponding to it. The agreement away from the origin is very good while deviations close to the origin suggest the use of the fully non-linear solution.

In the particular case of $k = \mp 1$, corresponding to the boundary between the region discussed above, the solution is

$$G_k(\xi) \sim \operatorname{sgn} \left(-\frac{1}{2}\xi \right)^{1/2} \quad \text{as } \xi \rightarrow -\infty \tag{4.7}$$

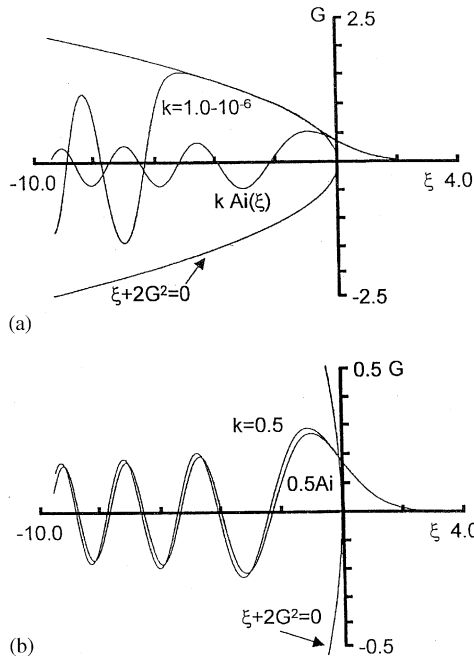


Fig. 3. Comparison of approximate solutions of Eq. (4.1) and exact solutions (numerical): (a) Comparison of numerical solution for $k = 1.0 \cdot 10^{-6}$ with $k Ai(\xi)$; (b) Comparison of solution for $k = 0.5$, the approximate non-linear solution in Eq. (4.4) with the Airy function asymptotic solution in Eq. (4.2), $k Ai(\xi)$.

which is the particular solution which corresponds to the Thomas–Fermi solution found by Dalfovo et al. [15] and further discussed by Lundh et al. [21]. In addition, if $|k| > 1$, $G_k(\xi)$ has a pole at a finite value of ξ , say ξ_0 , depending on k , with

$$G_k(\xi) \sim \text{sgn}(k)(\xi - \xi_0)^{-1} \quad \text{as } \xi \downarrow \xi_0. \tag{4.8}$$

The solution in Eq. (4.7) represents a nodeless wavefunction and hence can be associated with the ground state of the problem. Consequently, it received special attention in the literature [15,21]. The oscillatory solutions in Eq. (4.4) all possess nodes and they correspond to large amplitude spatial fluctuations of the condensate close to its boundary. This should not be confused with small perturbations around the nodeless ground state solutions which have been investigated separately in the literature [22].

We will discuss the physical relevance and experimental support for these solutions in the Conclusions section. It is physically acceptable that these solutions lead asymptotically to zero both at $\xi \rightarrow \infty$ and $-\infty$. To make sure that this is the case we have calculated several physical properties of these solutions such as: normalisation (or equivalently the number of particles), N_k , the potential energy due to the external field, $(PE)_{field}$, the potential self energy, $(PE)_{self}$, and the solution’s kinetic energy, (KE) . Note that these quantities refer strictly speaking only to the vicinity of the boundary region where the approximation holds. However, for the sake of convenience they have

been defined in the infinite integration limit since the required cutoff values may depend on the case considered. These quantities are given by

$$\begin{aligned}
 \text{(a) } N_k &= \int_{-\infty}^{\infty} |\psi|^2 dx, \\
 \text{(b) } (\text{PE})_{field} &= \int_{-\infty}^{\infty} Fx|\psi|^2 dx, \\
 \text{(c) } (\text{PE})_{self} &= \int_{-\infty}^{\infty} U_0|\psi|^4 dx, \\
 \text{(d) } (\text{KE}) &= \int_{-\infty}^{\infty} \left[-\frac{\hbar^2}{2m} \psi^* \frac{d^2\psi}{dx^2} \right] dx, \tag{4.9}
 \end{aligned}$$

which, when the scaling relations are used, become

$$\begin{aligned}
 \text{(a) } N_k &= b^2 \delta \int_{-\infty}^{\infty} |\phi|^2 dx, \\
 \text{(b) } (\text{PE})_{field} &= F\delta^2 b^2 \int_{-\infty}^{\infty} y|\phi|^2 dy, \\
 \text{(c) } (\text{PE})_{self} &= U_0 b^4 \delta \int_{-\infty}^{\infty} |\phi|^4 dy, \\
 \text{(d) } (\text{KE}) &= -\frac{\hbar^2}{2m} \frac{b^2}{\delta} \int_{-\infty}^{\infty} \phi^* \frac{d^2\phi}{dy^2} dy. \tag{4.10}
 \end{aligned}$$

Fig. 4A illustrates how the normalisation constant N_k depends on the parameter k that labels the particular solution.

Fig. 4B shows the dependence of $(\text{PE})_{field}$ on k , while Fig. 4C is a plot of $(\text{PE})_{self}$ with respect to k .

We have also investigated the spatial extent of the condensate’s boundary region and, since there are no generally predetermined cut-offs for these solutions, we propose to define the linear size of the condensate’s boundary region for a given function using the quantum equivalent of a standard deviation for a given value of k , i.e., (and this is shown in Fig. 5 for two choices of the limits of integration):

$$L_k = \left[\frac{2F\delta^2 b^2 \int_{-\infty}^{\infty} y^2 \phi_k^2(y) dy}{N_k} \right]^{1/2}, \tag{4.11}$$

where we have labelled the solutions $\phi_k(y)$ with the index k introduced earlier.

Note that each diagram contains two curves obtained from integrating the formulas in Eq. (4.10) with two different lower limits of integration. This is consistent with the definition of the variable, x , and its finite range in the negative direction signifying the radial size of the condensate’s boundary region. In the positive direction there

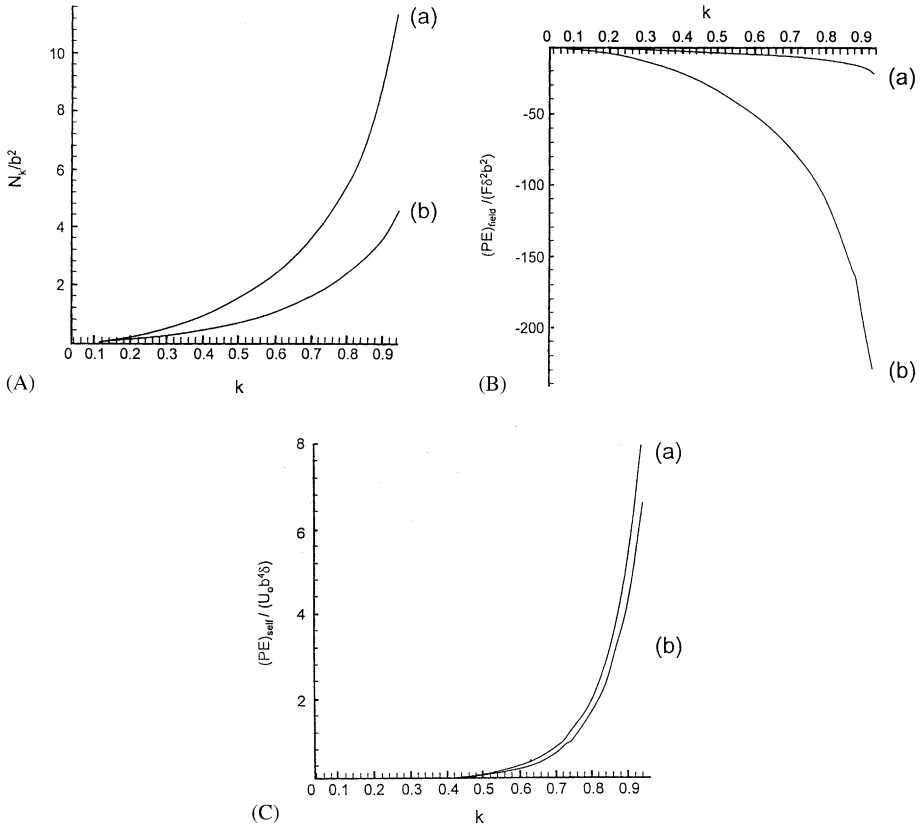


Fig. 4. (A) The scaled normalisation parameter, N_k/b^2 versus k for: (a) an integration range $-60 < \xi < +60$ and (b) an integration range $-10 < \xi < +10$. (B) $(PE)_{field}/F\delta^2b^2$, versus k , for: (a) an integration range $-10 \leq \xi \leq +10$ and (b) an integration range $-60 \leq \xi \leq +60$ (C) $(PE)_{self}/(U_0b^4\delta)$, versus k , for: (a) an integration range $-60 \leq \xi \leq +60$ and (b) an integration range $-10 \leq \xi \leq +10$.

is no limitation on the values of x . However each of the solutions involved tends asymptotically to the same Airy function in Eq. (4.3) which, in turn, drops rapidly to zero giving an insignificant contribution to the integrals in question. The diagrams presented show a dependence of the five quantities listed in terms of the parameter k that labels members of the Painlevé II family. Note that as $k \rightarrow 1$ the solution approximates the nodeless ground state field and in the opposite limit as $k \rightarrow 0$ the amplitude decreases to zero whilst the frequency of oscillations continuously increases. With this information we now discuss the results of the numerics. Fig. 5 indicates clearly that increasing the value of k enlarges the size of the condensate and the nodeless solution therefore contains the largest possible number of particles within an available region of space. Furthermore, extending the lower limit of integration also leads to a dramatic increase in the normalisation coefficient, N_k , the latter function being monotonic in k . Fig. 4B demonstrates how the external confining potential lowers the potential

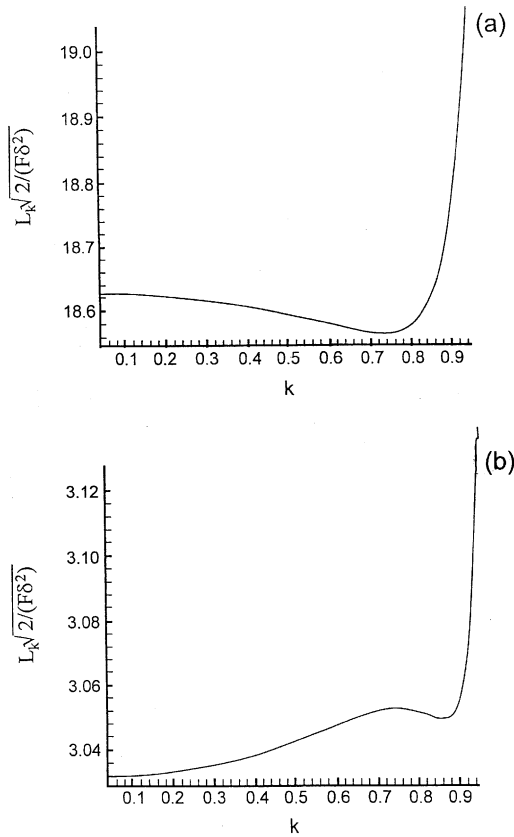


Fig. 5. Scaled linear size of the condensate, $L_k \sqrt{2/(F\delta^2)}$, versus k , for integration ranges (a) $-60 \leq \xi \leq +10$, (b) $-10 \leq \xi \leq +10$.

energy with an increasing value of k . This is again a monotonic function of k and it also experiences a dramatic drop as the lower limit of integration is extended. The self-energy i.e., the energy of the condensate’s interacting particles, rapidly increases with the value of k but not significantly with the lower limit of integration, which is somewhat unexpected—see Fig. 4C. Finally in Fig. 5 we have plotted how the size of the condensate’s boundary region depends on k . It appears that the size, L_k , initially decreases with k and then exhibits a dramatic upturn close to $k = 0.8$. It also appears that there may be more than one state, as defined by k , giving the same size. A possibility exists that the ground state and an excited state have the same size and be energetically close. This statement is consistent with some experimental findings [7]. Finally, when making comparison with physical systems, the scaling factors in both the dependent and independent variables should be carefully evaluated. Having investigated the possibility of not just a single nodeless state as a representation of the Bose condensate but the existence of a family of wavefunctions with nodes, we wish to pursue the question of their stability.

5. Stability considerations

The issue of stability is closely linked to that of the condensate’s excitation spectra. When a condensate is weakly disturbed by sinusoidal perturbations, it will oscillate with characteristic frequencies which can be both theoretically and experimentally determined. This is provided the condensate’s wavefunction is stable. The theoretical procedure starts with a stationary solution of the GP equation to which is added a small perturbation in terms of normal modes of the quasi-particle excitations [23]. The obtained formula in the Bogoluibov form [24] reads

$$(\hbar\omega)^2 = \left(\frac{\hbar^2 q^2}{2m}\right) \left(\frac{\hbar^2 q^2}{2m} + 2gn\right), \tag{5.1}$$

where \mathbf{q} is the wavevector of the excitation and $n = 1\phi^{12}$ is the density of the gas. For large momentum the spectrum coincides with the free particle energy $\hbar^2 q^2/2m$ [24]. It is remarkable, that in spite of no adjustable parameters in the formula, it predicts excitation frequencies with a 2% accuracy when compared to the experimentally measured values for the Rubidium 87 condensate. Our intention in this section is much less ambitious. First of all we wish to determine if the large amplitude oscillations analysed in the previous section possess global stability. Secondly we intend to determine if small perturbations to these solutions can be found in the form of bound states which would highlight stability against small perturbations. In Fig. 6(a) we have plotted the family of solutions corresponding to e.g. (4.4) for a range of values of k . This is very reminiscent of fundamental harmonics on a string except the amplitude decreases as the independent variable, ξ , tends to $-\infty$. Nonetheless it is reasonable to expect that at least marginal stability of these solutions i.e., perturbing them transforms one solution into its phase-space neighbour. This is indeed borne out by the contour plot analysis shown in Fig. 6(b) where the same solutions as those in Fig. 6(a) are represented in Poincaré section. The contour plots resemble concentric circles characteristic of a harmonic oscillator. These curves are naturally more complicated than circles but the basic property is very similar. To further substantiate this claim we have perturbed these fully non-linear solutions by small excitations and obtained an eigenvalue equation

$$-\chi'' + (\xi + 2G_k^2)\chi = E\chi, \tag{5.2}$$

where $G_k(\xi)$ belongs to the family given in Eq. (4.4). We have numerically solved the above Schrodinger equation for a range of k ’s between 0 and 1 and have found the presence of negative-eigenvalue bound states in all cases. For the benefit of the reader we provide two extreme cases for $k=0.001$ in Fig. 7 and for $k=0.999$ in Fig. 8. Each panel in these figures shows a consecutive bound state starting with a ground state and gives the corresponding eigenvalue. Each excited state differs from the previous one by an extra node. It is clear therefore that the family of damped oscillatory solutions presented in this paper possesses desirable physical characteristics i.e., (a) convenient normalisation for the condensate’s size, (b) finite energy, (c) absence of singularities

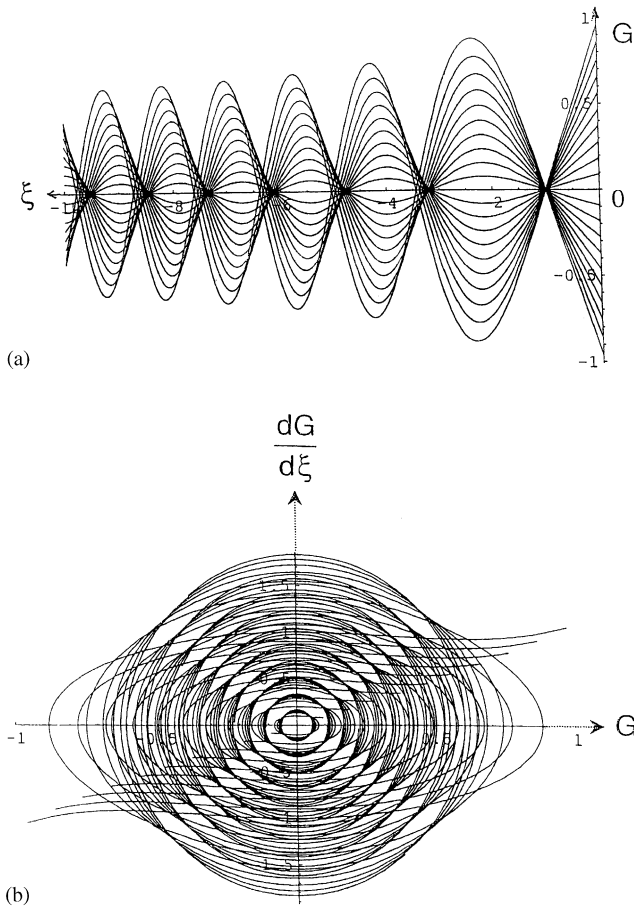


Fig. 6. (a) A plot of the family of functions $G(\xi)$ in Eq. (4.4) and (b) the corresponding contour plot.

and, as demonstrated in this section, global stability in the sense of large perturbations transforming one solution into another and stability against small perturbations which can become bound states with the square of the condensate’s wavefunction playing the role of an effective potential.

Whilst the linear ramp potential afforded some analytical insights the parabolic potential equation is not integrable and must therefore be attacked numerically.

6. A parabolic spherically symmetric trap

In the linear ramp potential the quasi-one-dimensional analytical and numerical investigations pointed to the existence of an oscillatory region in the condensate’s wavefunctions close to the condensate’s boundary. We suspect that these solutions survive

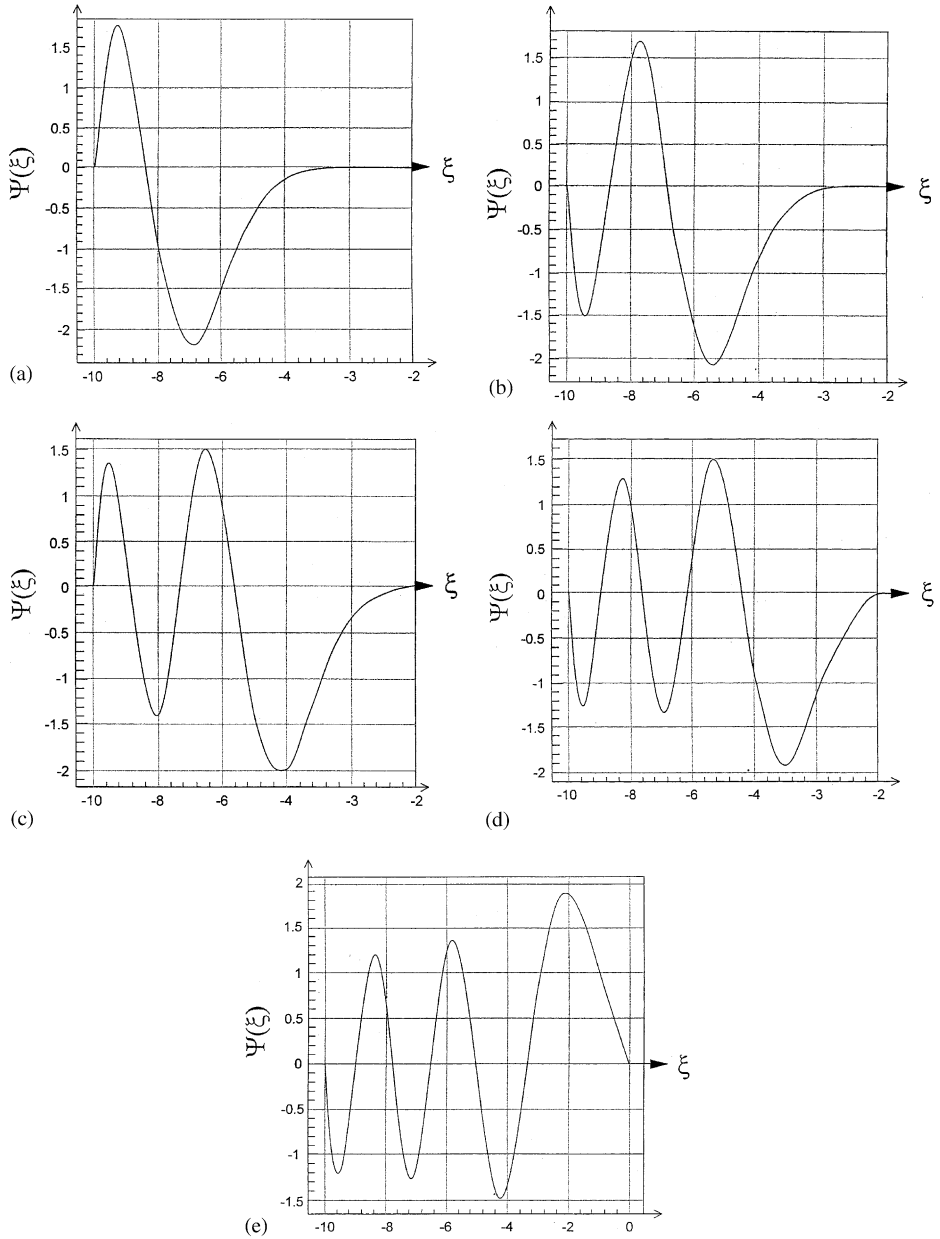


Fig. 7. The five lowest lying bound states in Eq. (5.2) for $k = 0.001$. $E =$ (a) -5.9091 ; (b) -4.4732 ; (c) -3.2030 ; (d) -2.0379 ; and (e) -0.9142 .

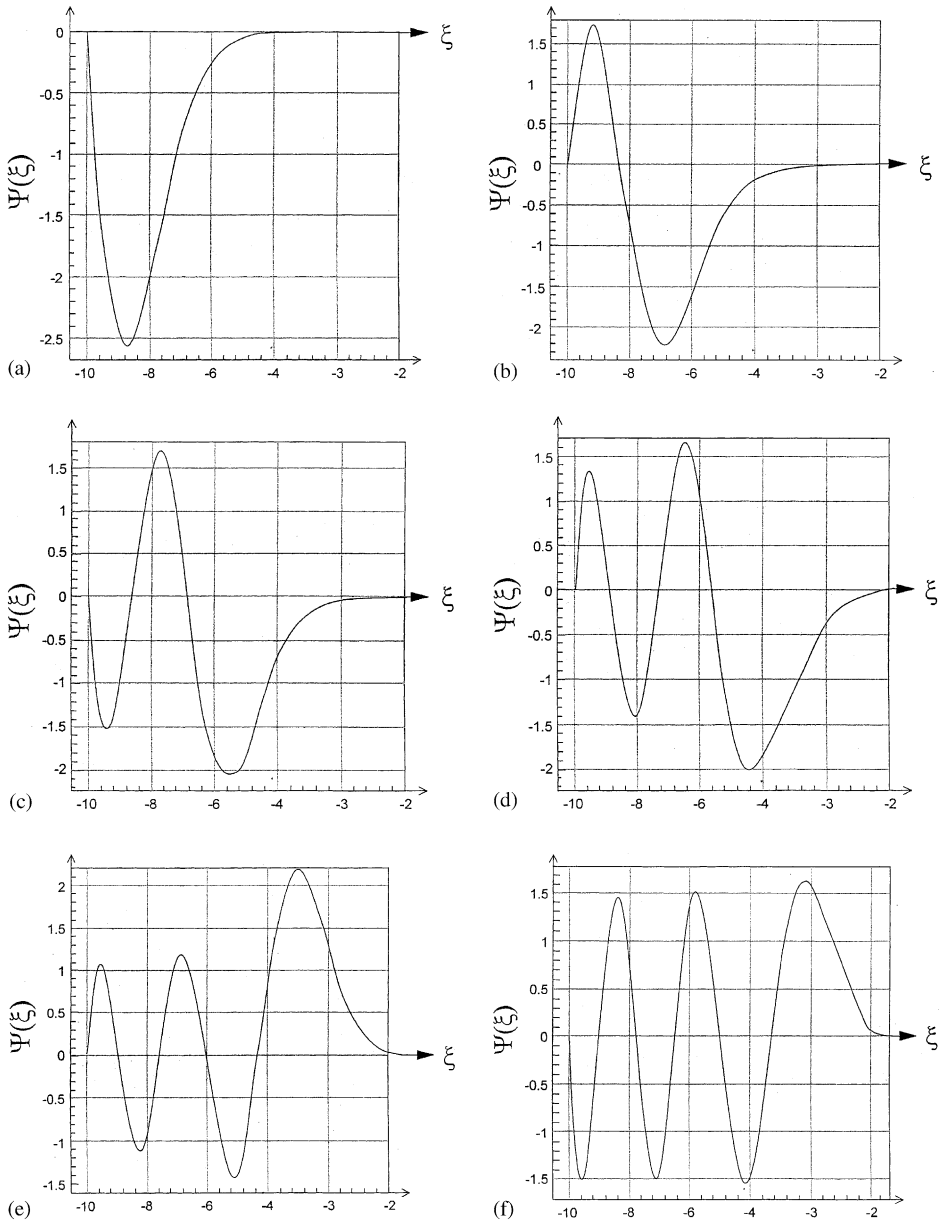


Fig. 8. The six lowest lying bound states in Eq. (5.2) for $k = 0.999$. $E =$ (a) -7.3196 ; (b) -5.5387 ; (c) -4.0717 ; (d) -4.0717 ; (e) -1.6164 and (f) -0.3687 .

in the parabolic potential for a fully three-dimensional solution in spherical symmetry. Further indications can be found in a recent paper by Kivshar and Alexander [25] in the parabolic 1D approximation as well as in the quasi two-dimensional trap. In all cases non-linear wavefunctions with several nodes were found. However, the nodeless solution appears to have the lowest energy in all cases. Similarly to our findings in the previous section, several nodes have been found corresponding to the same normalisation.

In this section we analyse numerically solutions of the GP equation in 3D with radial symmetry and in the presence of a parabolic potential, i.e.,

$$\phi_{rr} + \frac{2}{r}\phi_r + (\beta - r^2)\phi - \sigma\phi^3 = 0, \quad (6.1)$$

where $\phi_r = d\phi/dr$. We use the attendant norm

$$N = 4\pi \int_0^\infty \phi^2 r^2 dr \quad (6.2)$$

and the energy, H , given by

$$H = 4\pi \int_0^\infty \left(\phi_r^2 + r^2\phi^2 + \frac{\sigma\phi^4}{2} \right) r^2 dr. \quad (6.3)$$

The amplitude of the nodeless ground state depends on the parameter β , which is basically the chemical potential that determines the size of the condensate. Increasing the size of the non-linearity parameter, σ , with a fixed β , reduces the amplitude of the ground state. In Fig. 9 we illustrate the first excited state with one node on each side of the origin and $\sigma=1$. Fig. 10 compares the profile of the ground state amplitude with $\beta=3$ and $\sigma=+1$ to the first excited state's amplitude with $\beta=7$ and $\sigma=+1$ as their peak value is virtually the same. Fig. 11 shows the dependence of the peak of the ground state's amplitude for a selected set of values of β as a function of the non-linearity strength, σ . All these curves exhibit a dramatic drop in the amplitude in the range of σ 's which then tapers off for $\sigma > 0.25$. In Fig. 12 we have plotted the norm, N , against the normalised chemical potential for the ground state and, for comparison, the first excited state. Lastly Fig. 13 we show how the dimensionless Hamiltonian functional varies with the norm, N , for both the ground and first excited state when $\sigma=+1$.

7. Discussion and conclusion

In this paper we have investigated the existence of multimode wavefunctions that characterise a Bose–Einstein condensate under specific conditions near the boundary. These functions were obtained as exact solutions of the GP equation in the linear ramp approximation and are described as Painlevé II Transcendents. There are both theoretical and experimental indications that these large amplitude condensate spatial fluctuations may play a role in various manifestations of the Bose-condensation

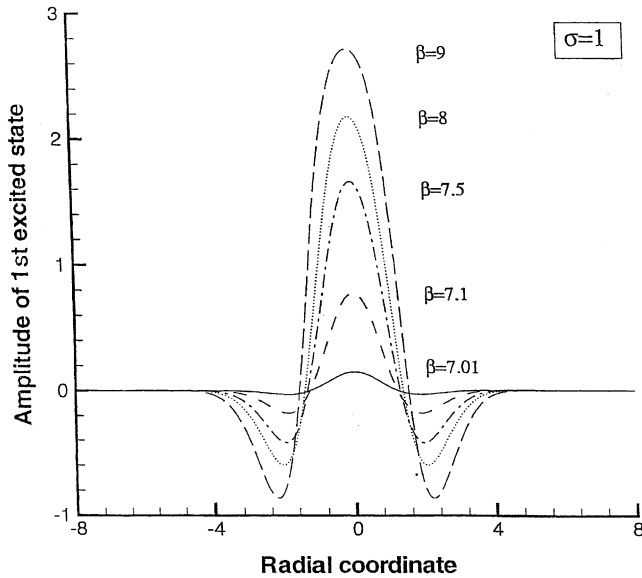


Fig. 9. The amplitude of the first excited state amplitude in 3D versus the radial co-ordinate, r , as a function of β with the non-linearity parameter, σ , fixed at $\sigma = 1$.

phenomenon and are not merely an artefact of the approximation adopted. Further numerical work by Kivshar and Alexander [25] shows that these states also emerge in the case of a condensate in a two-dimensional parabolic potential. Our numerical work in the spherically symmetric condensate for a parabolic trap clearly indicates the persistence of oscillatory states. It also appears that in all cases investigated the ground state is nodeless. This remains to be rigorously proved using functional analysis methods for our non-linear GP equation with a general confining potential. We have also investigated the stability of these solutions being fully aware that even exact solutions lose their physical appeal if they are unstable against perturbations. Firstly contour plots in the phase plane showed this family of Painlevé Transcendents as concentric closed curves filling a large region within the allowed parameter space. This indicates that when globally perturbed these large amplitude condensate excitations deform one into another member of the family somewhat reminiscent of standing wave harmonics. To further convince ourselves of their stability we have investigated their behaviour under small perturbations. A linearised Schrodinger equation with an effective potential in the form of the squared excitation function was solved numerically for a range of allowed parameters, k . We have found bound state solutions in all cases examined in the entire range of allowed values of k (although we have reported only on the extreme values). Conforming to a typical expectation each higher excited state has an extra node and a negative eigenvalue. It is noteworthy that earlier numerical studies of Bose condensates [26], described by a variant of the non-linear Schrodinger equation, reported the existence of oscillatory solutions which could not be eliminated.

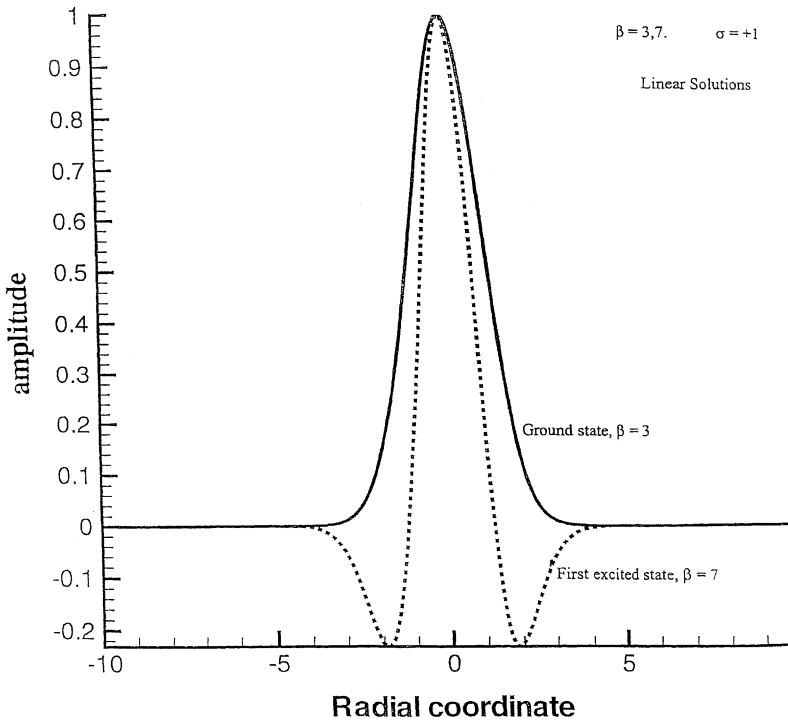


Fig. 10. A comparison of the 3D ground state amplitude profile for $\beta = 3$ and $\sigma = +1$ with the first excited state's amplitude for $\beta = 7$ and $\sigma = +1$.

Perhaps a more pressing issue is related to the experimental evidence for such states. In terms of Bose–Einstein condensates in atomic gases trapped magnetically we wish to point to the work of Bradley et al. [7] who found highly oscillatory profiles of the absorption cross-section in a laser beam which was used as a probe to measure the number and temperature of the trapped atoms. Even more direct evidence for such states (as many as 8 excited states were observed) has been supplied in the study of Bosonic quantum dots [27]. These are spatially confined submicrometre superconducting samples whose properties vary greatly with their size and exhibit behaviour, due to size quantisation of the Cooper pair motion. The resulting transitions between discrete states, resembling our excited states of the condensate, have been observed in a magnetic field [27]. Furthermore, these authors were able to observe regimes of stability for the condensate's excited states with a net non-zero angular momentum quantised to $L = 0-2$. This, of course, suggests a natural extension of the present theoretical investigation in which a fully non-linear analysis is carried out for the GP equation in spherical symmetry with a non-zero angular momentum, i.e., to analyse solutions of

$$i\phi_t = \nabla^2 \phi + \left[\alpha + \beta r^2 + \frac{L(L+1)}{r^2} \right] \phi + J\phi^3 . \tag{7.1}$$

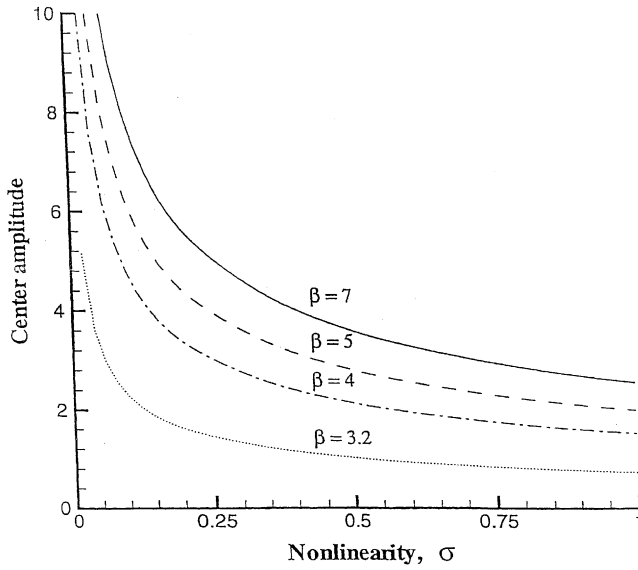


Fig. 11. The dependence of the peak of the 3D ground state's amplitude as a function of the nonlinearity parameter, σ , for a selected set of values of β .

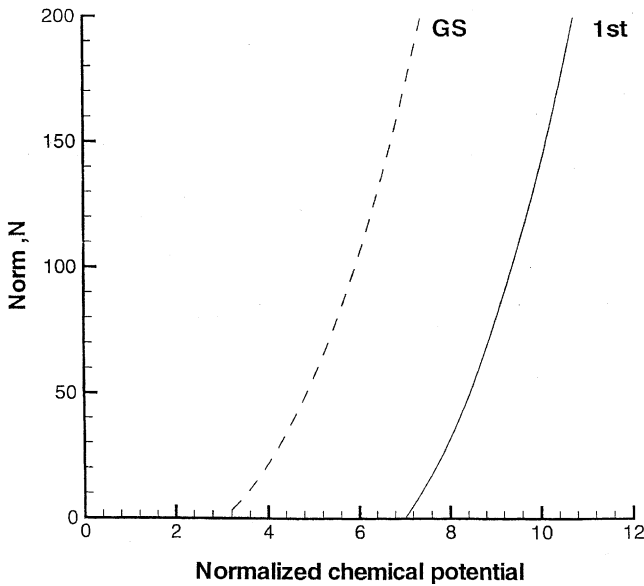


Fig. 12. A plot of the norm, N , against the normalised chemical potential for the ground and first excited states in 3D.

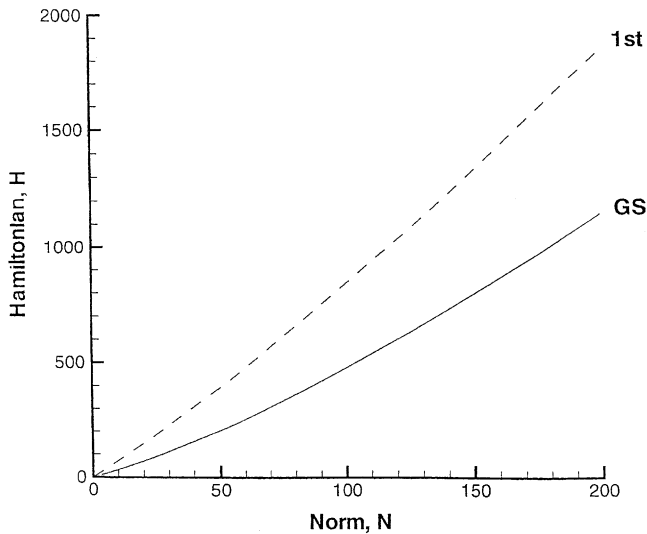


Fig. 13. The Hamiltonian functional versus the norm, N , for $\sigma = +1$ in 3D.

We intend to pursue this problem in the near future in the context of the emergence of a Yrast line in the energy spectrum of weakly interacting trapped bosons [28,14].

The large amplitude excitations discussed in this paper may also be related to the experimental observations on ^3He and ^4He thin films. In particular the inferred probability density profiles for ^3He [29,30], for several coverages behave in a very similar manner to the spatial co-ordinates. Lastly, recent experiments [31,32] allowed the observation of condensate length oscillations as a function of time. These oscillations were generated by first modulating the magnetic trapping potential to excite the condensate. Periodic changes in both length and width were observed on a millisecond timescale and a μm length scale. Such large scale fluctuations can easily be attributed to the large amplitude density fluctuations exhaustively analysed in the present paper.

Acknowledgements

This research was supported by grants from NSERC, the Royal Society, NATO and the Danish Research Council. J.A.T. and P.L.C. wish to thank Professor B. Mottelson for drawing their attention to this problem and to Dr. C.J. Pethick for his valuable comments and literature on the topic. J.M.D. wishes to thank the staff of the Theoretical Physics Institute for their kindness and thoughtfulness during his stay. J.A.T. and J.M.D. express their gratitude to Professor Peter Clarkson for providing them with the references concerning Painlevé Transcendents and equations. Both J.A.T. and M.S. express their gratitude to members of the Institute of Mathematical Modelling at the D.T.U. for their hospitality during their visit.

References

- [1] S.N. Bose, *Z. Phys.* 26 (1924) 176.
- [2] A. Einstein, *Sitzungsber. Kgl. Preuss. AkadWiss.* 1924 (1924) 261;
A. Einstein, *Sitzungsber. Kgl. Preuss. AkadWiss.* 1925 (1925) 3.
- [3] F. London, *Nature* 141 (1938) 643;
F. London, *Phys. Rev.* 54 (1938) 947.
- [4] E.C. Svensson, V.F. Sears, in: D.F. Brewer (Ed.), *Progress in Low Temperature Physics*, Vol. XI, North-Holland, Amsterdam, 1987, p. 189.
- [5] M.H. Anderson, J.R. Ensher, M.R. Matthews, C.E. Wieman, E.A. Cornell, *Science* 269 (1995) 198.
- [6] K.B. Davis, M.-O. Mewes, M.R. Andrews, N.J. van Druten, D.S. Dufree, D.M. Kurn, W. Ketterle, *Phys. Rev. Lett.* 75 (1995) 3969.
- [7] C.C. Bradley, C.A. Sackett, R.G. Hulet, *Phys. Rev. Lett.* 78 (1997) 985;
C.C. Bradley, C.A. Sackett, J.J. Tollet, R.G. Hulet, *Phys. Rev. Lett.* 75 (1995) 1687.
- [8] D.S. Jin, J.R. Ensher, M.R. Matthews, C.E. Wieman, E.A. Cornell, *Phys. Rev. Lett.* 77 (1996) 420;
M.-O. Mewes, M.R. Andrews, N.J. van Druten, D.M. Kurn, D.S. Durfee, C.G. Townsend, W. Ketterle, et al., *Phys. Rev. Lett.* 77 (1996) 988.
- [9] C.G. Townsend, et al., in: *Proceedings of the 15th International Conference on Atomic Physics*, Amsterdam, 1996.
- [10] E.P. Gross, *Nuovo Cimento* 20 (1961) 454;
E.P. Gross, *J. Math. Phys.* 4 (1963) 195.
- [11] L.P. Pitaevskii, *Zh. Eksp. Teor. Fiz.* 40 (1961) 646.
- [12] J.M. Dixon, J.A. Tuszynski, P.A. Clarkson, *From Nonlinearity to Coherence*, Oxford University Press, Oxford, 1997.
- [13] R.K. Dodd, J.C. Eilbeck, J.D. Gibbon, H.C. Morris, *Solitons and Nonlinear Wave Equations*, Academic Press, London, 1982.
- [14] G.F. Bertsch, T. Papenbrock, *Phys. Rev. Lett.* 83 (1999) 5412.
- [15] F. Dalfovo, L.P. Pitaevskii S. Stringari, *Phys. Rev. A* 54 4213.
- [16] P.A. Clarkson, J.B. McLeod, *Arch. Rat. Mech. Anal.* 103 (2) (1988) 97–138.
- [17] R.R. Rosales, *Proc. Roy. Soc. Lon. A* 361 (1978) 265–275.
- [18] P.A. Clarkson, J.B. McLeod, Painlevé transcendents their asymptotics and physical applications, in: P. Winternitz, D. Levi (Eds.), *Proceedings, Ste Adèle, Quebec, Canada, September 1990*, Plenum, New York, 1990.
- [19] E.L. Ince, *Ordinary Differential Equations*, Dover, New York, 1956.
- [20] S.P. Hastings, J.B. McLeod, A boundary value problem associated with the second Painlevé transcendent and the Kortweg-de Vries equation, *Arch. Rat. Mech. Anal.* 73 (1980) 31–51.
- [21] E. Lundh, C.J. Pethick, H. Smith, *Phys. Rev. A* 55 (1998) 2126.
- [22] M. Edwards, et al., *Phys. Rev. Lett.* 77 (1996) 1671;
D.S. Jin, et al., *Phys. Rev. Lett.* 77 (1996) 420.
- [23] F. Dalfovo, S. Giorgini, L.P. Pitaevskii, S. Stringari, *Rev. Mod. Phys.* 71 (1999) 463.
- [24] N. Bogolubov, *J. Phys. USSR* II (1947) 23.
- [25] L. Berge, T.J. Alexander, Yu.S. Kivshar, *Phys. Rev. A* 62 (2003) 023 607.
- [26] C.A. Jones, S.J. Putterman, P.H. Roberts, *J. Phys. A* 19 (1986) 2991.
- [27] A.K. Gevin, S.V. Dubonos, J.G.S. Lok, M. Henini, J.C. Maan, *Nature* 396 (1998) 144;
A.K. Gevin, I.V. Grigorieva, S.V.I. Dubonons, J.G.S. Lok, J.C. Maan, A.E. Filippov, F.M. Peeters, *Nature* 390 (1997) 259.
- [28] B. Mottelson, *Phys. Rev. Lett.* 83 (1999) 5412.
- [29] D.S. Sherrill, D.O. Edwards, *Phys. Rev. B* 31 (1985) 1338.
- [30] E.M. Krotschect, *Phys. Rev. B* 32 (1985) 5713.
- [31] D.M. Stamper-Kurn, et al., *Phys. Rev. Lett.* 81 (1998) 500.
- [32] D.S. Jin, et al., *Phys. Rev. Lett.* 78 (1997) 764.